

Preservation of total phenolic content (TPC) in cucumber juice concentrate using non-thermal Progressive Freeze Concentration: Quantitative design characteristics and process optimization

Nur Nabilah Hanani Mohd Rosli^a, Noor Hafiza Harun^a, Roshanida Abdul Rahman^a,
Norzita Ngadi^a, Shafirah Samsuri^c, Nurul Aini Amran^c, Nor Zanariah Safiei^d,
Farah Hanim Ab Hamid^e, Zaki Yamani Zakaria^a, Mazura Jusoh^{a,b,*}

^a School of Chemical Engineering, Faculty of Engineering, Universiti Teknologi Malaysia, 81310, Skudai, Johor, Malaysia

^b Centre of Lipids Engineering and Applied Research (CLEAR), Universiti Teknologi Malaysia, 81310, Skudai, Johor, Malaysia

^c Chemical Engineering Department, Universiti Teknologi PETRONAS, Seri Iskandar, 32610, Perak, Malaysia

^d Food Engineering Technology Section, Universiti Kuala Lumpur Malaysian Institute of Chemical & Bioengineering Technology, Taboh Nanning, 78000, Alor Gajah, Melaka, Malaysia

^e School of Chemical Engineering, College of Engineering, Universiti Teknologi MARA, Selangor, Malaysia

ARTICLE INFO

Handling Editor: Cecilia Maria Villas Bôas de Almeida

Keywords:

Cucumber juice
Freeze concentration
Crystallization
Optimization
Non-thermal

ABSTRACT

Progressive freeze concentration (PFC) was used to concentrate cucumber juice to preserve total phenolic content (TPC) in this work as a non-thermal process. Since the productivity of PFC is always an issue, this work aimed to carefully fabricate an ice crystallizer with quantified design characteristics and optimized for an effective cucumber juice concentration process. A new device called Multiple Probe Cryo-Concentrator (MPCC) was designed, and to quantitatively identify the PFC design characteristics, the improvement in ice crystallization surface area coupled with appropriate apparatus shape factor and mixing power consumption were first calculated. From these analyses, it was observed that the improved surface area of the MPCC has given 35.44% improvement in terms of productivity and excellent fluid movement provided by the shape factor and mixing power consumption. With the aid of central composite design (CCD), the PFC operating parameters were then optimized to obtain the most effective values of effective partition constant, K -value (0.381) and TPC increment (30.13%) using multi-response optimization. The achieved optimum conditions included operation time of 35 min, initial concentration of 6 mg/ml, coolant temperature of -10.7 °C and stirrer speed of 400 rpm. From the regression modelling analysis and graphical plots, it was found that the stirrer speed has the most significant impact towards solute concentration in cucumber juice. In overall, it is evident that the design characteristics of the apparatus play an important role in giving a better PFC performance. Optimizing the PFC system for better efficiency can successfully maximize the nutritional properties, simultaneously indicating its high practicality in other fruit or vegetable juice concentration.

1. Introduction

Cucumber or *Cucumis sativus* juice contains a diverse range of nutrients such as protein, fat, carbohydrates, and also some essential vitamins (Agatemor et al., 2018). Published data also revealed that it possesses various medicinal properties like antioxidant, antimicrobial, antibacterial, antifungal, anti-carcinogenic, anti-inflammatory, antifertility, antiaging, antidiabetic and efficacy in lowering cholesterol level (Kumar et al., 2017). The responsible active constituents are flavonoids,

saponins, tannin, steroids and alkaloids with different compositions at different parts of the cucumber (Mallik and Akhter, 2012; Saidu et al., 2014). Flavonoids, the largest group of naturally occurring phenolic compounds that can fight against cardiovascular diseases and cancers (Abbas et al., 2017; Basli et al., 2017; Lutz et al., 2019), is the most popular anti-oxidant mainly present in cucumber juice (Chandra et al., 2014). It can be reflected by the total phenolic content (TPC) measured in the juice extracted best from its whole fruit, i.e., from its peel, flesh and seed (Yunusa et al., 2018).

* Corresponding author. School of Chemical Engineering, Faculty of Engineering, Universiti Teknologi Malaysia, 81310, Skudai, Johor, Malaysia.
E-mail address: mazura@cheme.utm.my (M. Jusoh).

<https://doi.org/10.1016/j.jclepro.2021.129705>

Received 31 January 2021; Received in revised form 31 October 2021; Accepted 11 November 2021

Available online 13 November 2021

0959-6526/© 2021 Elsevier Ltd. All rights reserved.

Suitable to be grown in temperate and tropic climate, the cucumber production is relatively sustainable in tropical regions throughout the world, where Asia countries (i.e., Thailand, China and Vietnam) is the largest producer (Jia and Wang, 2021). Cucumbers are creeping vine plants and easy to grow thus very prolific. In view of global industry of cucumber juice, the top-ranked import markets is led by countries of United States (i.e., \$558.47M import value in 2020), followed by Germany and Netherlands (<https://www.tridge.com>). To maximize consumption and pack phenolic compounds in a small volume of juice (TPC per volume) for further use in cosmeceutical, pharmaceutical, food and beverage industries, a concentration process for the juice is extremely needed. Currently, there are various concentration techniques used in the fruit and vegetable juice industry categorized into thermal and non-thermal processing (Bhattacharjee et al., 2019; Bevilacqua et al., 2017).

The evolution of the juice concentration processes to find the best is shown in Fig. 1. Evaporation is the most common and frequently applied thermal process but it may lead to the loss of color, flavor, aroma, nutritional value, and taste of the concentrated juice due to the use of high temperatures (Liu et al., 2020), on top of the high cost for energy consumption (Fellows, 2017). Non-thermal concentration processes like reverse osmosis (RO) bring minimally modified sensory, nutritional, and functional properties of the juice (Bevilacqua et al., 2017; Bhattacharjee et al., 2019). RO is a pressure-driven membrane separation technology which entails the movement of water against concentration gradient through a membrane (Rastogi, 2016). However, it is unable to achieve higher degree of concentration compared to evaporation due to high osmotic pressure limitation and membrane fouling with the soluble materials in the solution on the external surface or within the pores of the membrane (Rastogi, 2016; Bevilacqua et al., 2017).

To overcome shortcomings of all the mentioned techniques, freeze concentration (FC) has been used and it can attain higher quality and healthier juice concentrates. FC is a non-thermal process that removes water content in a solution by freezing it into ice crystals at subzero temperature, which is very suitable for thermally sensitive fruit juices including cucumber (Samsuri et al., 2016). The concept is to form and grow high-purity ice crystals which expel the impurities, hence producing a concentrated liquid in the end (Miyawaki et al., 2016).

As can be seen in Fig. 1, FC technique can be classified into two main categories: (i) systems with homogenous ice nucleation (ii) systems with heterogenous ice nucleation. FC with homogenous nucleation is

categorized into block FC and suspension FC, and generally will take a long operation time just to induce the first ice nucleus and costly due to complex ice crystal growth and ice crystal separation (Liu et al., 1999; Miyawaki and Inakuma, 2020). The block FC (freezing-thawing) will also require multiple cycles of operations due to its limitation in concentration efficiency hence requiring high energy consumption (Miyawaki and Inakuma, 2020). FC with heterogeneous ice nucleation induces the nucleation on cooled surfaces and is more popularly termed progressive FC (PFC). PFC produces a single large ice crystal that is formed layer by layer on a cooled surface (Samsuri et al., 2016). This provides easier separation of the ice block on the cooled surface from the concentrated liquid. However, PFC process efficiency has always been found to be lower than SFC (Samsuri et al., 2016), and this is a major setback to be overcome to enable successful commercialization. Thus, the objective of this study is to design a new ice crystallizer for a PFC system with quantified design characteristics to ensure improvement in terms of productivity as well as to provide the optimum condition for the most effective water removal for cucumber juice concentration through this type of non-thermal process.

In order to do this, focus was given to the design of the PFC system, to provide the largest surface area possible for ice nucleation and growth, added with an efficient solution/fluid movement to avoid solute inclusion in the ice formed while maintaining high process productivity. The ice crystallization surface area can influence the productivity of the process and concentration mechanism at the ice-liquid interface (Miyawaki et al., 2005). Table 1 shows some recent research on PFC with various designs of the cooled surface. To date, there is no work with the cooled surface designed as probes immersed in the target solution as highlighted in gray in Fig. 1.

In this research, a new apparatus was designed with a set of multiple probes immersed in a stirred tank and is called multiple probe cryo-concentrator (MPCC). The probes were designed in such a way to provide largest surface area possible for contact between the cooled surface and the solution. This was quantitatively assessed by comparing the surface area provided by MPCC to the conventional PFC setup.

In terms of fluid movement, generally in PFC, solution movement can be categorized into bulk flow (e.g.: tubular, cylindrical, spiral finned, vertical finned), film flow (e.g.: cylindrical, plate) and stirred/rotation. In MPCC, stirred/rotation movement was employed, thus the design characteristic of the apparatus related to efficient and adequately powerful stirring motion needs to be proven and detailed out to show its

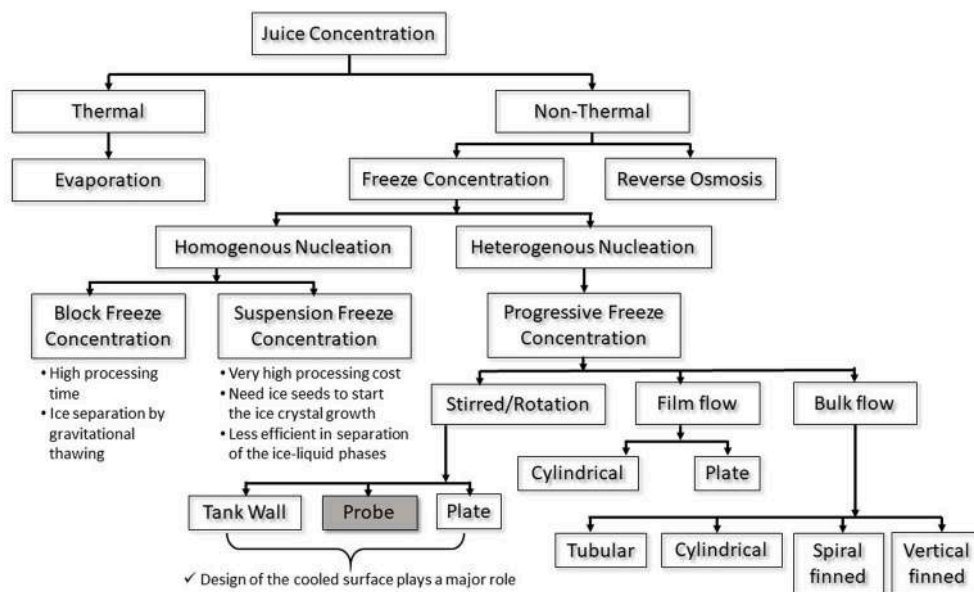


Fig. 1. Evolution of juice concentration processes.

Table 1
Summary of existing PFC design and their limitations.

Crystallizer	Application	Processing Parameter	Cooled surface design	Author
Multi-plate freeze concentration	Glucose, sucrose and fructose solution with simulated juice	<ul style="list-style-type: none"> Initial concentration, Various zone, Time operation 	Plate	Gulfo et al. (2013)
Spiral finned crystallizer	Concentrate orange juice, glucose solution	<ul style="list-style-type: none"> Coolant temperature Time operation, Circulation flowrate, Shaking speed 	Bulk flow - Cylindrical with spiral fins	Samsuri et al. (2015)
Vertical finned crystallizer	Concentrate apple juice	<ul style="list-style-type: none"> Coolant temperature, Circulation flowrate 	Bulk flow - Cylindrical with vertical fins	Amran et al. (2016)
Vertical placed tubular ice system	Apple juice	<ul style="list-style-type: none"> Coolant temperature, Speed circulation pump 	Bulk flow-tubular wall	Miyawaki et al. (2016)
Vacuum-assisted block freeze concentrator	Red wine	<ul style="list-style-type: none"> Time freezing Freezing temperature 	No solution movement	Petzold et al. (2016)
Stabilization tank and scrape surface refrigerator	Cabernet Sauvignon grape berries	<ul style="list-style-type: none"> Freezing temperature, Time Circulation 	Stirred tank – inner wall	Wu et al. (2017)
PFC with stirrer	Orange peel waste, biodiesel, wastewater	<ul style="list-style-type: none"> Drying temperature, Coolant temperature, Cooling time, Stirring rate 	Stirred tank – inner wall	Isa et al. (2019)
Intelligent freeze concentrator	Concentrate apple juice	<ul style="list-style-type: none"> Coolant temperature, Agitation speed 	Suspension freeze concentrator – no cooled surface	Ding et al. (2019)
Centrifugation-assisted freeze concentration	Blueberry juice	<ul style="list-style-type: none"> Temperature Time 	Block FC	Santana et al. (2020)

competency.

Following the design characteristics explored, determination of the optimum operating parameters of coolant temperature, stirrer speed, operation time and initial concentration of cucumber juice was carried out using response surface methodology (RSM), to achieve the most effective performance of the designed MPCC system. PFC productivity was observed based on effective partition constant (K -value) and the total phenolic content (TPC) increment, which were exploited as responses.

2. Materials and methodology

The methodology for this investigation is divided into two parts which are (2.1) Progressive Freeze Concentrator Design Characteristics, and (2.2) Progress Freeze Concentration Process Optimization. Each part will have its respective sub-methodology detailed explanations.

2.1. Progressive Freeze Concentrator Design Characteristics

2.1.1. MPCC design

The multiple probes cryo-concentrator (MPCC) was designed to concentrate cucumber juice based on the working principle and ice crystallization theories for a PFC process. It was inspired by several procedures in the technology development of ice crystallizer proposed by Bermingham et al. (2000). The MPCC setup mainly consists of a set of multiple probes, cylindrical stainless-steel solution tank (0.1 cm thickness), and jacketed with ethylene glycol-water solution as the coolant. Thus, the solution in the tank can be maintained close to the freezing temperature (at 2 °C). Polyurethane foam was used as insulator on the most outer surface layer of the tank to avoid the disturbance of the surrounding temperature towards system. A motorized stirrer was attached at the bottom of the tank (Kashid et al., 2011). The hollow probe set of 5 were made of stainless steel and supplied with coolant gas (i.e., R22) in the inside (hollow part). The probes are built in the same

size, where each probe has a diameter of 2 cm and 15 cm in length as shown in Fig. 2. The probe set was installed at the top of the tank to perform the concentration process and it is capable to rotate at 180° inter-directively to provide suitable distribution of the solution at the interface while keeping away the solutes from being entrapped in the produced ice. Refrigerant was supplied using a copper tube to provide cooling to the immersed probe when ice crystallization was performed in the solution (Wang et al., 2013). To represent one of the design characteristics for this MPCC, ice crystallization surface area was first calculated and the improvement compared to the conventional PFC setup by Liu et al. (1997) is presented.

2.1.2. Calculations of shape factor and impeller power consumption

Out of great concern on the design key factors that will affect the stirring characteristic, shape factor calculation and determination of impeller power consumption for the mixing process occurring as a result of the motion of the stirrer attached at the bottom of the solution tank were first done (McCabe et al., 2001). Fig. 3 shows the detailed dimension and structure of the stirrer (paddle impeller) as well as the level of cucumber juice in the solution tank. Selection of a well-mixed tank for PFC with the aim to provide laminar condition is needed for effective mass and heat transfers between the target solution and the coolant. This could lead to achieving high mixing efficiency and low energy consumption of the PFC process.

The Reynold number (Re) was determined in order to assess the mixing flow behavior as expressed in Equation (1) (McCabe et al., 2001). Consequently, note that mixing power is a function of shape factor (i.e., density is not a factor) and should be in laminar mixing regime of $Re < 200$ (unbaffled tank, paddle impeller), the mixing power (P) and specific power consumption (P/V) can be assessed by Equation (2) (Xie et al., 2011).

$$Re = \frac{N_i D^2 \rho}{\mu} \quad (\text{Equation 1})$$

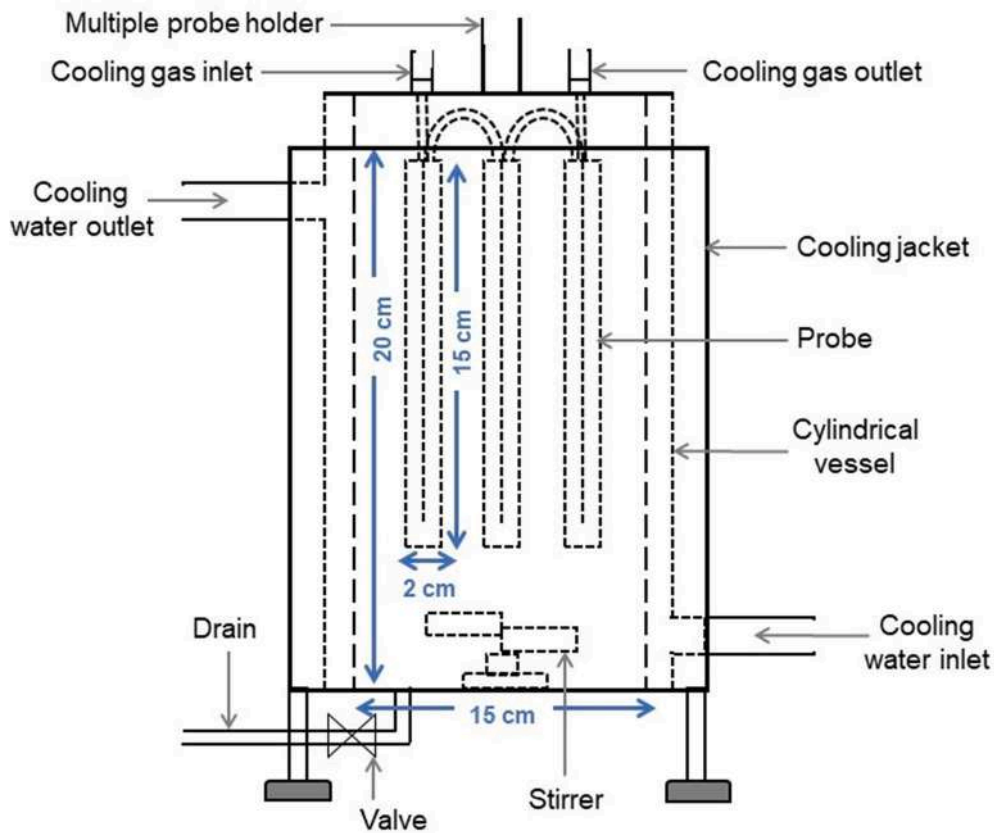


Fig. 2. Schematic diagram of multiple probe cryo-concentration system.

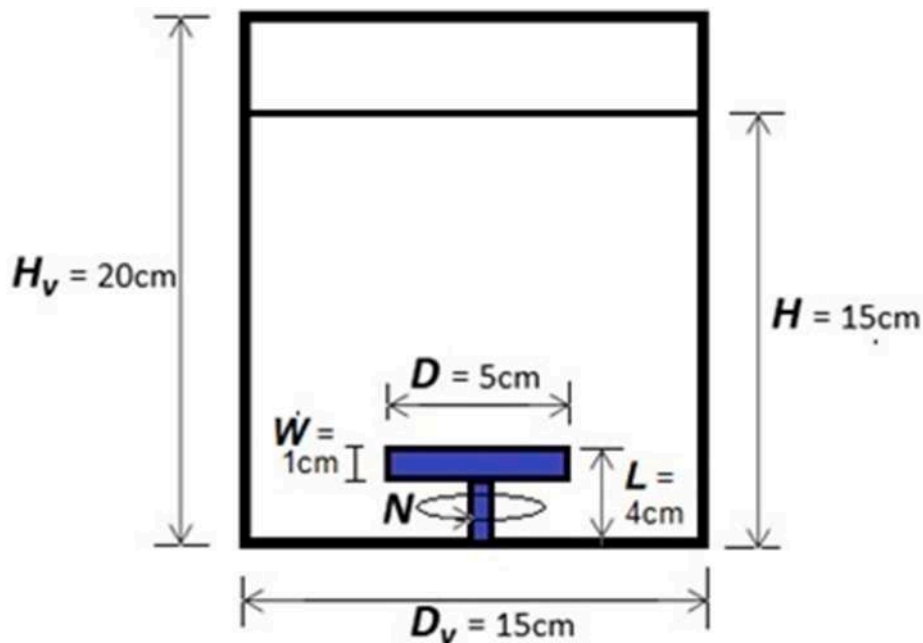


Fig. 3. Dimension of the stirrer and solution tank.

$$P = K_L \mu N_i^2 D^3$$

(Equation 2)

where N_i is the angular velocity, D is the impeller diameter, ρ is the solution density, μ is the solution viscosity and K_L is the mixing constant for laminar flow. Table 2 shows the information needed for impeller

power consumption calculation.

2.2. Progressive Freeze Concentration process optimization

2.2.1. Materials

This research was carried out using fresh cucumber juice, purchased

Table 2
Detailed information for the calculation of impeller power consumption.

Parameter	Formula	Detailed
Angular velocity	N_i	200 rpm = 3.3333 rev/s 250 rpm = 4.1667 rev/s 300 rpm = 5 rev/s 350 rpm = 5.8333 rev/s 400 rpm = 6.6667 rev/s
Density	$\rho;$	1060 kg/m ³
Viscosity	μ	0.12 Pa s
Diameter impeller	D	0.05 m
K_L	-	36.5
Working volume	V	0.003 m ³

from a local supermarket (Maslee Express) in Johor, Malaysia. Selection of good quality of cucumbers was made based on consistency of color and shape. The cucumbers were then subjected to the preparation activities of washing with distilled water, cutting into slices, and extracting the juice using a fruit juicer machine. The juice was stored at a temperature close to freezing point of pure water. Ethylene glycol (50%, v/v) of analytical grade was used as coolant liquid, purchased from Merck (Germany). Folin-Ciocalteu reagent and anhydrous sodium carbonate (Na₂CO₃) powder for spectrophotometry measurements were procured from Sigma-Aldrich (USA).

2.2.2. PFC experimental procedure

First, the cooled cucumber juice (2 °C) was placed in the tank at a volume of 3000 ml. Ethylene glycol-water coolant was then supplied into the jacketed wall of the solution tank to maintain the juice at 2 °C. Next, the probe set (i.e., MPCC) was immersed in the solution and rotated at 180° inter-directively. On the other hand, the stirrer speed was set in the range of 250–400 rpm to maximize the ice formation on the outer surface of the probes, as well as to form a well-mixed solution (Liu et al., 1999). The refrigerant was then set to the desired value, i.e., between temperature of -14 to -6 °C. When cooling is adequate, the ice crystals will start to develop on the outer surface of the probes and a concentrated cucumber juice will be left behind in the tank. The experiments were carried out according to the desired operating

conditions by manipulating parameters of cooling rate, stirrer speed, duration and initial concentration of juice solution. A thermocouple (data logger TC-08) was used to measure the solution temperature, and the data obtained were measured by online monitoring (Picolog software) throughout the experimental process. The concentrated solution of cucumber was eventually collected and the layer of ice crystal was thawed. An overview of the PFC work is illustrated in Fig. 4 and the procedure was done in triplicate for reproducible results.

2.2.3. Experimental design: PFC optimization

A statistical experimental design using response surface methodology (RSM) was implemented to determine one set of optimal condition of cucumber juice concentration process for the best K -value and TPC increment. Since the dependent variables (responses) are equally important in this PFC system, multi-response optimization was carried out to determine optimum conditions and predicted values for the two responses based on the overall desirability function of 0.92. There were four numeric factors, namely coolant temperature (X_1), stirrer speed (X_2), operation time (X_3) and initial concentration (X_4) generated and coded as presented in Table 3. The range of parameters studied was based on preliminary screenings (coolant temperature, operation time), literature findings (initial concentration) and limitations of the apparatus (stirrer speed) (Yahya et al., 2019; Samsuri et al., 2018). A set of 26 runs were repeated in triplicate according to the design matrix of central composite design (CCD). The experiments were conducted at five levels with two repetitions and axial point (at selective $\alpha = 2.0$) on two responses of K -value and TPC increment. Design Expert software (version 6.0.4, Stat-Ease, Inc.) was used for statistical analysis of the data

Table 3
Experimental range and coded value of variables.

Variables	Symbol	- α	-1	0	+1	$+\alpha$
Coolant temperature (°C)	X_1	-14	-12	-10	-8	-6
Stirrer speed (rpm)	X_2	250	300	350	400	450
Operation time (minute)	X_3	20	25	30	35	40
Initial concentration (mg/ml)	X_4	5	6	7	8	9

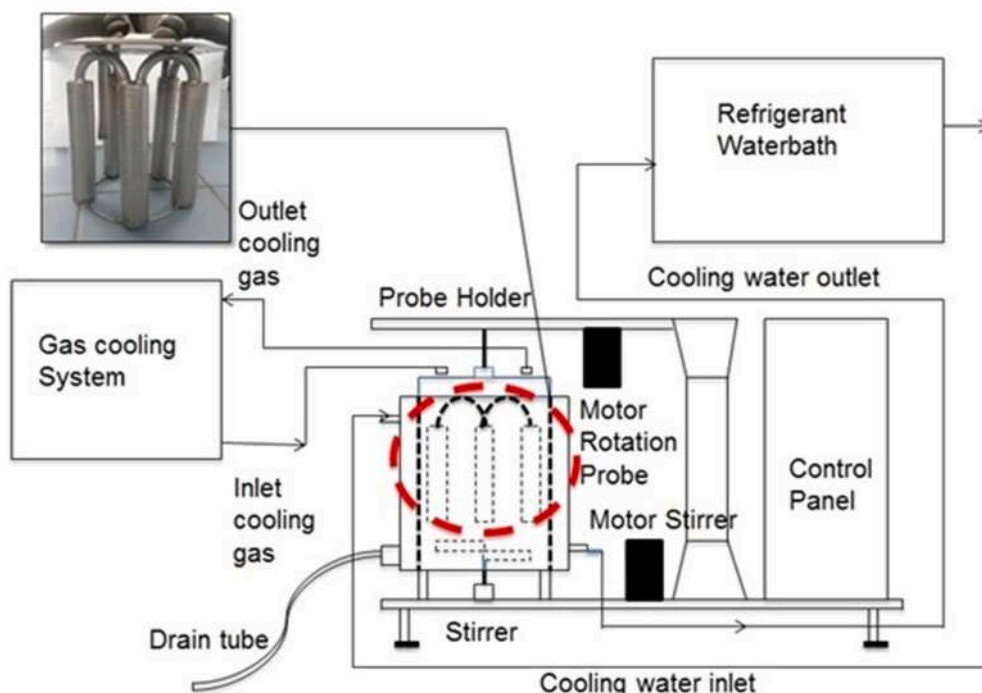


Fig. 4. Progressive freeze concentration using MPCC concentrator.

obtained with analysis of variance (ANOVA) of 95% reliability. A probability p-value (Prob > F) of lower than 0.05 was considered to be significant, while the model adequacy was also checked based on the F-value and the determination coefficient (R^2). The experimental data was then analyzed by multiple regression in order to fit the second order polynomial model as shown below.

$$Y = \beta_0 + \beta_1 X_i + \beta_2 X_i^2 + \beta_k X^k + \varepsilon \quad ; i = 1, 2, 3, 4 \quad (\text{Equation 3})$$

where Y is the response value predicted, β_0 is regression constant, $\beta_1, \beta_2, \beta_k$ are the coefficients of regression, X is experimental factor that influence the process, k is the degree of the polynomial, and ε is model error.

In addition, the substantive significance of statistical significance of the findings generated from the ANOVA was further determined by measuring the effect size. Thus, the eta-squared (η^2) was used to estimate the associated strength between variation based on variance-accounted-for. It is the ratio of sum of squares for the effect of interest to the total sum of squares, which is defined as follows (Levine and Hullett, 2002).

$$\eta_2 = SS_{\text{effect}} / SS_{\text{total}} \quad (\text{Equation 4})$$

where SS_{effect} is the sum of squares for the effect of interest, and SS_{total} is the total sum of squares for all effects, interactions and errors in the ANOVA.

2.2.4. Total phenolic compounds determination

Sample concentration used throughout the experiments was measured based on total phenolic content (TPC) using Folin-Ciocalteu method (Yunusa et al., 2018). Gallic acid was used for a standard calibration curve preparation, and the results were expressed as mg gallic acid equivalents (GAE) per 1 g of sample (mg GAE/g). Briefly, 1 ml of cucumber juice sample was mixed with 5 ml Folin-Ciocalteu reagent (10% (v/v)), and left for 10 min at room temperature. Then, 4 ml of Na_2CO_3 was added and kept in the dark for 45 min at temperature of 37 °C. After 30 min, the absorbance of sample was determined at wavelength 760 nm using UV-Vis Spectrophotometry (Mini UV 1240, Shimadzu, Japan).

2.2.5. Variables theoretical and measurement

In PFC system, the separation that occurs at the ice-liquid interface is crucial, represented by the effective partition constant (K -value), which acts as an effectiveness index of the freeze concentration process. Thus, the K -value being the ratio between concentration of solute in ice and concentrated solution was used to evaluate the PFC process efficiency as shown in the following equation (Samsuri et al., 2016; Liu et al., 1997).

$$K - \text{value} = C_s / C_L \quad (\text{Equation 5})$$

where C_s is the TPC concentration in the solid (or ice) and C_L is the TPC concentration in the liquid. K -value ranges between 0 and 1, and lower K -value indicates more effective PFC performance (Miyawaki et al., 2012).

In addition, antioxidant capacity in cucumber juice can be represented by percentage of TPC increment as a result of the PFC process applied (Safiei et al., 2016). Hence, this variable can be calculated by defining an amount of the TPC recovered in the concentrated liquid in relation to its initial concentration, as given in Equation (6).

$$\text{TPC increment} = \frac{M_{a,L} - M_{i,L}}{M_{i,L}} \times 100 \quad (\text{Equation 6})$$

where $M_{a,L}$ is the mass of TPC in the concentrated liquid (after) and $M_{i,L}$ is the mass of TPC in the initial solution (before).

3. Results and discussions

3.1. Improvement of ice crystallization surface area

As stated by Zhang and Liu (2018), heterogenous ice nucleation is often promoted by foreign bodies in solution tank such as surface (i.e., wall of tank or probe) and particle presence (i.e., solute). With the aim to have a relatively high surface area, a cylindrical tank shape and five hollow probes were used to justify the better improvisation in the newly designed of MPCC crystallizer. In conventional PFC method, only a single large ice crystal was grown gradually on the cooled surface (i.e., tank inner surface immersed in coolant) in vertical direction from the bottom of the cylindrical tank (Liu et al., 1997). Meanwhile, in this newly designed PFC, nucleation of ice crystal occurs heterogeneously on the outer surface of the probes entirely (i.e., MPCC) thus giving more spaces instead of only the portion of the inner wall immersed in the solution in the conventional setup. Therefore, the PFC apparatus dimension was carefully calculated to allow for ice progression between the probes, which could lead to high subsequent crystal growth and enhance the PFC efficiency. Table 4 shows the comparison of PFC apparatus measurements between MPCC crystallizer (Fig. 2) and a conventional cylindrical crystallizer taking the diameter of the cylindrical sample vessel (i.e., 7.5 cm) and its height to calculate maximum ice crystallization surface area (i.e., 20 cm). Thus, the maximum improvement of ice crystallization surface area for this study is 50.45%. Fig. 5 shows the ice formation around the probe in one of the experimental works.

If considering only the bottom of the vessel (cross-sectional area) in the conventional design for ice nucleation and growth, the increment of surface area would be incomparable (2,677%). To make a fairer comparison between the two designs, it should be noted that to provide the same surface area for ice nucleation as the MPCC (502.65 cm^2), the radius of the bottom surface of the vessel should be 12.5 cm, which is a 420% increment or 5.21-fold of the original diameter of the vessel. This also means that the coolant tank needs to be bigger than 25 cm in diameter to provide the setup, compared to only 15 cm for MPCC. This shows that the size of the space required to position the apparatus is 66.67% larger for the conventional design of the equivalent ice crystallization surface area. This strongly indicates that the MPCC is more attractive to be used practically.

Most importantly, to see improvement in terms of productivity, the maximum ice growth that can be provided by MPCC is 904.77 cm^3/h (at its most effective coolant temperature) compared to only 668.02 cm^3/h (at its maximum ice front growth rate) recorded by Liu et al. (1997), which is translated into 35.44% improved productivity. This clearly shows the MPCC design characteristic is far more superior than the conventional design.

3.2. Quantitative design characteristics (shape factor and power consumption)

In brief, the calculation of shape factor reflects the design characteristics that play important role in PFC process for the ice heterogenous nucleation and crystal growth. The dimensions formula and shape factor calculation as well as its standard ratio are shown in Table 5. It can be

Table 4
Comparison of apparatus measurements between MPCC and a conventional PFC.

Variable/Ice nucleation	5-probe set of MPCC crystallizer	Conventional cylindrical crystallizer (Liu et al., 1997)
Ice crystallization surface	outer wall of probes	bottom of sample vessel
Radius of surface	1 cm × 5 unit	2.4 cm
Height of surface	15 cm	19.75 cm
Surface area (max)	502.65 cm^2	334.01 cm^2 (max)



Fig. 5. An improvement of ice crystallization surface area using MPCC.

Table 5
Shape factor description and calculation.

Shape factor	Standard Ratio	Descriptions	Calculated MPCC Shape Factor
S1	$D_v/D = 3$	Tank diameter/impeller diameter	15 cm/5 cm = 3
S2	$H/D = 0.75 - 1.3$	Height of impeller above vessel floor/Impeller diameter	4 cm/5 cm = 0.8
S3	$L/D = 1$	Length of impeller blade/Impeller diameter	5 cm/5 cm = 1
S4	$D/W = 0.2$	Impeller diameter/Width of blade	5 cm/1 cm = 0.2
S5	$H/D_v = 0.8 \sim 1$	Height of liquid/Diameter of tank	15 cm/15 cm = 1
S6	$H_v/D_v = 1.3$	Height of tank/Diameter of tank	20 cm/15 cm = 1.3

seen that the obtained/calculated values fit the standard ratio for listed for the tank geometry thus proving that this element of the MPCC was well designed to perfectly mix the cucumber juice solution. The ratios describe a formula to standardize the combination of tank with stirrer that can substantially influence flow patterns and mixing performance in PFC process. Thus, a careful selection of tank design characteristics is therefore important, which will certainly affect the fluid motion and subsequently the quality of the final product.

Since the design characteristics also have a strong impact on energy requirement, mixing power and impeller power consumption for PFC system were determined by using Equations (3) and (4). The Re was measured as 147.22 (i.e., <200), which confirmed the laminar flow of the cucumber juice solution behavior in the PFC system. Accordingly, the mixing power obtained was 24.33 Watt by taking the maximum stirrer speed at 400 rpm. Then, the calculated specific power consumption (P/V) of one run of PFC system was 8.11 kW/m³. Normally, power consumption per unit volume in industrial bioreactors ranges from 10 kW/m³ for small vessel and 1–2 kW/m³ for large vessel (McCabe et al., 2001). Thus, the P/V of PFC system using MPCC crystallizer indicated conclusively that it is still economic and could reduce the energy requirement. Depending on the PFC efficiency that is being performed, selection of better design characteristics in concentrating

cucumber juice is highly crucial as the apparatus shape factor dictates the energy cost of the system.

3.3. Process optimization

According to CCD experiments, the independent and dependent parameters were well tabulated in Table 6. The obtained results of K-value ranged from 0.296 to 0.895, while TPC increment varied from 13.30 to 30.93.

3.3.1. Process optimization models

This study was targeting to improve the concentration performance as well as to provide better productivity of cucumber concentrate. RSM was used to predict the optimum values that represent the highest process efficiency. Two responses were well-fitted to the second-order polynomial equations. Through ANOVA (Table 7), the correlation coefficient (R²) values obtained for K-value and TPC increment were 0.988 and 0.969, respectively. The respective mathematical models for each response are shown in Equations (7) and (8) below:

Effective partition constant, K-value:

$$Y_1 = 4.163 + 0.177X_1 - 0.0011X_2 - 0.131X_3 - 0.054X_4 + 0.017X_1^2 - 0.000002X_2^2 + 0.0001X_3^2 + 0.007X_4^2 + 0.0004X_1X_2 + 0.0001X_1X_3 + 0.005X_1X_4 + 0.0002X_2X_3 - 0.0003X_2X_4 + 0.0006X_3X_4 \tag{Equation 7}$$

Table 6
CCD arrangements for PFC experiments.

Run	Initial Concentration (mg/ml)	Speed of Stirrer (rpm)	Coolant Temperature (°C)	Operation Time (minutes)	Effective Partition Constant, K-value	TPC Increment
1	7	350	-10	30	0.552	24.06
2	8	400	-12	35	0.489	26.15
3	6	400	-8	25	0.502	28.79
4	6	400	-12	25	0.402	27.79
5	8	400	-8	35	0.664	19.74
6	7	350	-10	20	0.675	24.17
7	6	300	-8	35	0.492	19.21
8	9	350	-10	30	0.723	22.47
9	7	350	-10	40	0.498	29.18
10	7	250	-10	30	0.802	18.81
11	6	300	-12	35	0.562	25.89
12	6	300	-12	25	0.81	20.51
13	7	450	-10	30	0.296	28.52
14	7	350	-14	30	0.836	18.96
15	5	350	-10	30	0.48	26.25
16	8	400	-8	25	0.562	24.15
17	8	300	-12	25	0.895	21.64
18	6	300	-8	25	0.767	18.05
19	8	300	-8	25	0.861	15.24
20	6	400	-12	35	0.393	30.93
21	8	400	-12	25	0.452	24.53
22	8	300	-8	35	0.743	20.38
23	7	350	-6	30	0.866	13.30
24	8	300	-12	35	0.774	29.12
25	6	400	-8	35	0.469	26.68
26	7	350	-10	30	0.552	24.06

Table 7
Regression coefficients and ANOVA of second-order polynomial model for K-value and TPC increment.

Factor	K-value						TPC Increment					
	SS	DF	MS	F-value	p-value	η^2	SS	DF	MS	F-value	p-value	η^2
Model	0.73	14	0.052	67.19	<0.0001**		507.24	14	36.23	24.21	<0.0001**	
<i>Linear term</i>												
X_1	0.005	1	0.005	6.31	0.0289*	0.00676	86.79	1	86.79	58.00	<0.0001**	0.1657
X_2	0.37	1	0.37	477.37	<0.0001**	0.50000	140.84	1	140.84	94.12	<0.0001**	0.2689
X_3	0.043	1	0.043	55.71	<0.0001**	0.05811	31.33	1	31.33	20.94	0.0008**	0.0598
X_4	0.097	1	0.097	125.42	<0.0001**	0.13108	24.93	1	24.93	16.66	0.0018**	0.0476
<i>Quadratic</i>												
X_1^2	0.084	1	0.084	108.19	<0.0001**	0.11351	57.90	1	57.90	38.69	<0.0001**	0.1106
X_2^2	0.0007	1	0.0007	0.84	0.3790 ^{ns}	0.00095	0.068	1	0.068	0.046	0.8349 ^{ns}	0.0001
X_3^2	0.0002	1	0.0002	0.24	0.6346 ^{ns}	0.00027	11.59	1	11.59	7.75	0.0178*	0.0221
X_4^2	0.0009	1	0.0009	1.10	0.3158 ^{ns}	0.00122	0.97	1	0.97	0.65	0.4368 ^{ns}	0.0019
<i>Interactions</i>												
X_1X_2	0.026	1	0.026	32.86	0.0001**	0.03514	12.67	1	12.67	8.47	0.0142*	0.0242
X_1X_3	0.00002	1	0.00002	0.023	0.8816 ^{ns}	0.00003	19.89	1	19.89	13.29	0.0038**	0.0380
X_1X_4	0.002	1	0.002	1.98	0.1866 ^{ns}	0.00270	5.69	1	5.69	3.80	0.0772 ^{ns}	0.0109
X_2X_3	0.046	1	0.046	59.38	<0.0001**	0.06216	27.35	1	27.35	18.28	0.0013**	0.0522
X_2X_4	0.004	1	0.004	4.67	0.0535 ^{ns}	0.00541	31.19	1	31.19	20.85	0.0008**	0.0596
X_3X_4	0.014	1	0.014	17.40	0.0016**	0.01892	0.32	1	0.32	0.21	0.6532 ^{ns}	0.0006
Residual	0.009	11	0.0008				16.46	11	1.50			
Lack of fit	0.009	10	0.009				16.46	10	1.65			
Total	0.74	25					523.70	25				
	CV,% = 4.50, $R^2 = 0.9884$, $R^2_{adj} = 0.9737$						CV,% = 5.23, $R^2 = 0.9686$, $R^2_{adj} = 0.9286$					

SS, DF, MS, CV and η^2 represent sum of squares, degree of freedom, mean square, coefficient of variation, and eta-squared, respectively.

Note: * Significant at $p < 0.05$; ** Significant at $p < 0.01$; ^{ns} Not significant at $p > 0.05$. The scales of effect size magnitudes are taken from Cohen’s guideline; ‘small’ at 0.01, ‘medium’ at 0.06, and ‘large’ at 0.14 (Cohen, 1988).

TPC increment:

$$Y_2 = -97.909 - 7.740X_1 + 0.472X_2 - 1.210X_3 + 1.618X_4 - 0.455X_1^2 + 0.00003X_2^2 + 0.033X_3^2 + 0.236X_4^2 + 0.009X_1X_2 - 0.112X_1X_3 - 0.298X_1X_4 - 0.005X_2X_3 - 0.028X_2X_4 + 0.028X_3X_4 \tag{Equation 8}$$

where Y_1 and Y_2 are the predicted values of the K -value and TPC increment, respectively. Meanwhile, X_1 , X_2 , X_3 and X_4 represent coolant temperature, stirrer speed, operation time and initial concentration, respectively.

3.3.2. Regression model verification

The regression modelling results for all responses are indicated in Table 7. It was found that each model demonstrates high significance with low probability of p -value (<0.0001) and high F -value. In addition, it is statistically acceptable due to the low values of the coefficient of the variation ($CV < 10\%$), which represents the dispersion degree of the data.

From Table 7, it can be concluded that linear terms of stirrer speed, operation time and initial concentration; and the quadratic term of coolant temperature are significant model terms for K -value at very small p -values (i.e. $p < 0.01$), compared to the linear effect of coolant temperature at the level of $p < 0.05$. Meanwhile, the quadratic effects of X_2^2 , X_3^2 and X_4^2 are insignificant at $p > 0.05$ for the K -value. For TPC increment, it can be statistically observed in ANOVA (Table 7) that all linear terms and quadratic effect of X_1^2 are highly significant at $p < 0.01$. Only the factor of X_3^2 is significant at $p < 0.05$, while other quadratic factors (i.e., X_2^2 and X_4^2) were found to be insignificant at $p > 0.05$. The interaction factors between independent variables and responses are discussed in detail in the following response surface contour plots.

3.4. Response surface plot analysis

Three-dimensional (3D) response surface plots were plotted for better visualization of each response variable at the optimum level. These interpretations were obtained against two variables to examine their interaction effects while the other two variables were held constant. Then, the relationships between the two independent variables were ascertained and discussed.

3.4.1. Effect of variables on effective partition constant, K -value

The independent variable of K -value represents the exclusion of solute from the advancing ice front through the concentration mechanism between phases. From Fig. 6, it can be seen that the stirrer speed has the most significant effect on K -value indicating the high stirring rate (i.e., <450 rpm) could lead to better efficiency of the concentration process. The K -value decreases when the stirrer speed increases, meaning that ice crystallization of cucumber juice is successfully progressed. This is in agreement with one reported study that K -value was strongly dependent on the stirring rate at the ice front and the advance rate of the ice front to produce high purity ice (Miyawaki et al., 1998). A slower solidification rate will occur when higher stirring speed is evenly applied, hence keeping solutes away from the ice-liquid interface, rapidly brought into the solution, thereby reducing the ice crystal inclusion (Liu et al., 1997; Samsuri et al., 2018). However, further increase in the stirring speed at

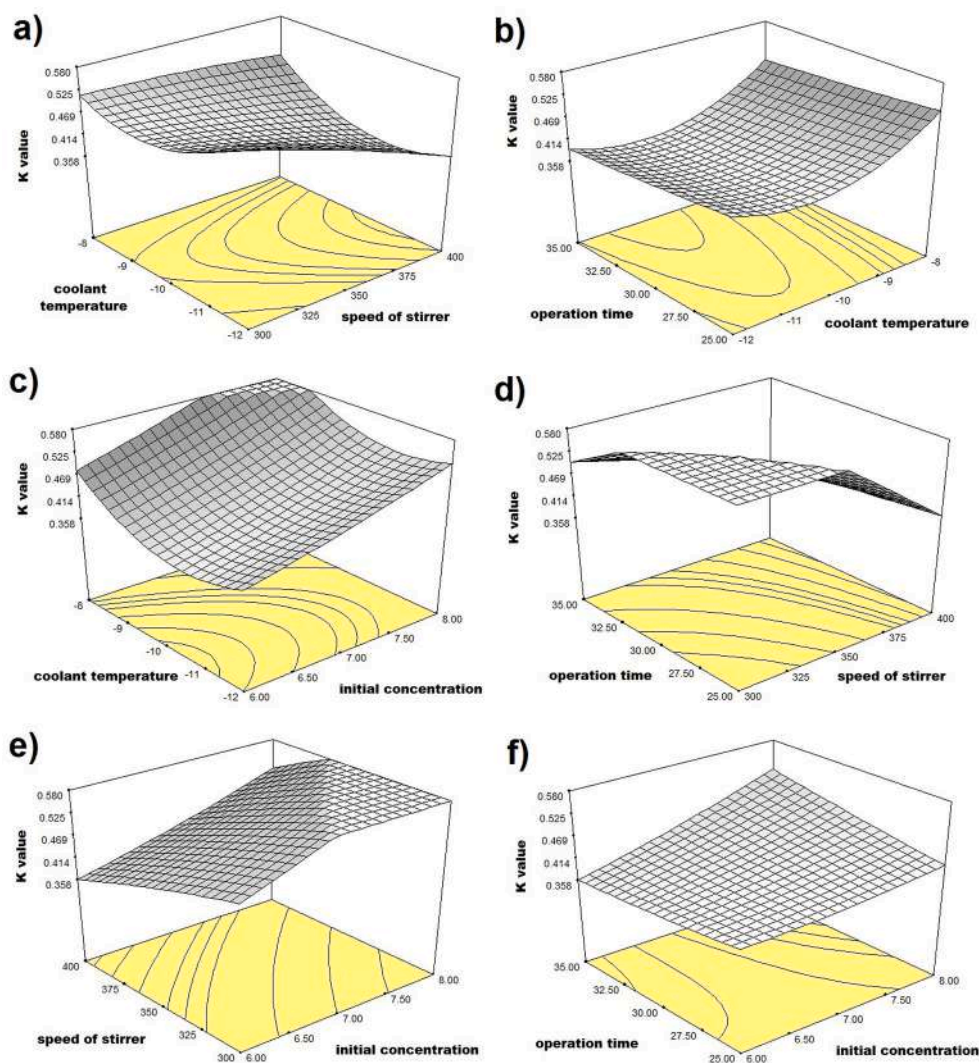


Fig. 6. Response surface plots for interactions between variables on K -value.

higher than 450 rpm should be avoided as the interface containing rejected solute and ice layer formed on the inner wall will erode, thus making the solution less concentrated where much pure water volume will return back to the solution (Hamid et al., 2015).

It can also be seen (Fig. 6a) that the stirrer speed and coolant temperature have strong interaction towards *K*-value. By increasing the stirrer speed at coolant temperatures ranging from -9 to -12 °C, low *K*-values are observed. However, *K*-value increases when the coolant temperature applied is higher than that region, and begins to sharply increase at temperature lower than -9 °C for all stirrer speed values. A higher *K*-value indicates a lower PFC efficiency. In the meantime, the strongest interaction effect between the stirrer speed and operation time is witnessed in Fig. 6d, in addition to highly significant *p*-value (<0.0001) obtained from ANOVA (refer Table 7). At constant coolant temperature of -10.7 °C and initial concentration of 6 mg/ml, the plots reveal that lower *K*-values are found at a stirrer speed higher than 400 rpm and operation time not more than 35 min. Meanwhile, from Fig. 6e, the lowest *K*-value is achieved at the highest stirrer speed and lowest initial concentration of solution.

Other than that, it can be observed that *K*-value has its lowest point (i.e., below 0.5) with decreasing initial concentration and in the range of -8 to -12 °C of coolant temperature. This condition is supported by the theory stated by Zhang and Liu (2018) where the ice formation rate is controlled by coolant temperature. The solute becomes easily trapped

when too low coolant temperature is applied and as a result, *K*-value increases. The trends of the plotted graph in Fig. 6b and c can be inferred as coolant temperature factor giving the highest impact on *K*-values (<0.5) within the range of -8 to -12 °C. Theoretically, the ice front growth rate is greatly dependent on the coolant temperature (Miyawaki et al., 1998). As noticed in Fig. 6, the higher growth rate at the lowest coolant temperature could lower the *K*-value, thus producing the higher ice purity. Meanwhile, in Fig. 6f, the interaction between operation time and initial concentration towards *K*-value revealed that higher operation time and lower initial concentration contribute to low *K*-values, indicating that high efficiency of the PFC system can be achieved at this operating condition. This is in line with one study reporting that a longer process time to form the ice on the probe's cold surface is due to the freezing point depression of the solution and the phenomenon of supercooling (Miyawaki et al., 2016).

Furthermore, eta-squared was used as a measure of effect size. It was found that stirrer speed had the highest effect on the *K*-value as given by highest linear eta-squared (0.50000), followed by initial concentration (0.13108), operation time (0.05811) and coolant temperature (0.00676). However, based on Cohen's guideline, only stirrer speed can be interpreted as giving large effects ($\eta^2 > 0.14$) on *K*-value showing that it has stronger differences between variables (Cohen, 1988). In the meantime, initial concentration, operation time and its interaction with stirrer speed produced medium effects ($0.06 < \eta^2 < 0.14$). All other

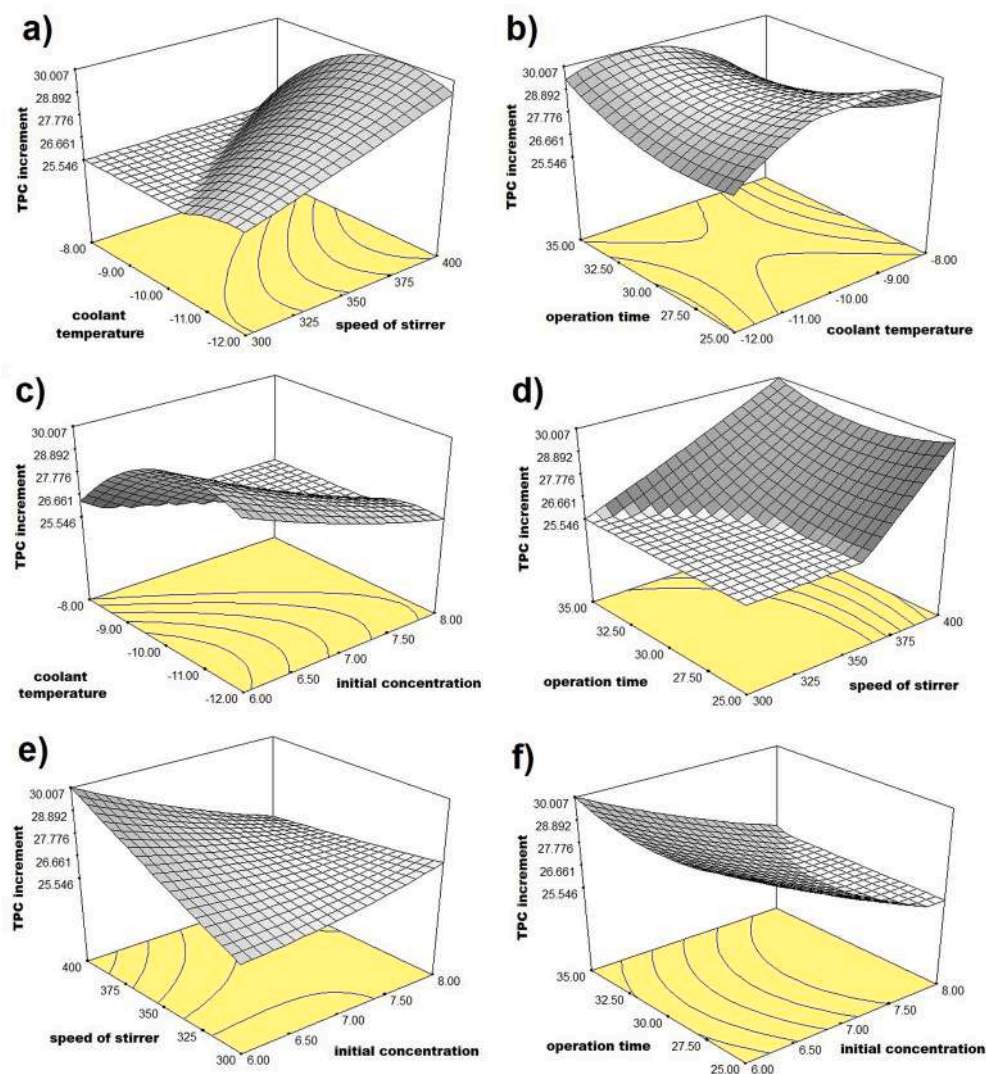


Fig. 7. Response surface plots for interactions between variables on TPC increment.

factors were found to have small or no effect on K -value.

3.4.2. Effect of variables on TPC increment

TPC increment in the cucumber juice concentrates embodies the purity of ice crystal in PFC process. Since preservation of bioactive compounds in the concentration is the main aim, the high retention TPC suits the best in describing the performance of this PFC system. Fig. 7 demonstrates the response interactions between the level of each factor towards TPC increment. From ANOVA (Table 7), even though the single effect of initial concentration is very significant, but its interaction effects with coolant temperature and operation are seemingly insignificant. Meanwhile, TPC increment is significantly affected by other interaction of variables at low p -values (i.e., $p < 0.05$ and $p < 0.01$).

From Fig. 7c, it can be observed that an adequate growth of ice crystals can be achieved at low initial solution concentration below than 7 mg/ml and coolant temperature ranging between -8 and -12 °C. The phenomenon of constitutional supercooling does not occur in this condition, thus dendritic ice crystal structure can be prevented in order to obtain the optimum TPC increment. In other words, freezing points and solution viscosity are the main variable that affect the PFC process (Auleda et al., 2011).

Meanwhile, the greatest TPC increment was observed at the lowest initial concentration and the highest stirrer speed as depicted in Fig. 7e. This is due to high shear force from the high liquid flowrate that could carry the solute away in the solution without being trapped in the ice layer formed. Likewise, the shear force could easily wash away the solutes trapped in the dendritic ice structure (Yahya et al., 2017). Other than that, the interactive effect of initial concentration and operation time on TPC increment is shown in Fig. 7f where the optimum condition can be found at initial concentration lower than 7.5 mg/ml and operation time higher than 30 min. These results are supported by a study discovering that the PFC concentration efficiency drops with increasing initial concentration due to increased solute content trapped in the ice crystal layer (Safiei et al., 2016). Briefly, as the initial concentration exceeded 7.5 mg/ml, TPC increment starts to decrease and is almost static, indicating the lower efficiency of the system.

From Fig. 7d and e, it can be observed that the stirrer speed interactions with operation time and initial concentration have high significant impact on TPC increment. The best condition falls above the stirrer speed of 350 rpm with an increase of other variables. However, if the stirrer speed applied were too high, it could end up as less concentrated solution due to erosion occurred. This is due to the facts that the solutes are kept away from the ice-liquid interface which gives enhancement of the heat transfers of the ice crystal (Samsuri et al., 2018). Thus, less inclusion of solute is achieved in the ice layer formed. Basically, the ice thickness formed is increased when operated with longer operation time, while the solid form of high ice purity can be obtained when high stirrer speed is applied. Eventually, it could wash away the solutes at the dendritic ice structure.

Meanwhile, Fig. 7a shows that the TPC increment increases when the stirrer speed is increased, and the best range for coolant temperature is approximately -12 to -10 °C. From Fig. 7b, the intermediate value of coolant temperature (i.e., -11 to -9 °C) yielded the best value of TPC increment in this interaction. Briefly, interactions of operation time with other variables seem to be insignificant as represented in Fig. 7b, d and 7f. Then, the mutual interactive behavior of coolant temperature and initial concentration can be observed in Fig. 7c, where the highest TPC increment is achieved at moderate ranges of coolant temperature and initial concentration lower than 7 mg/ml. A phenomenon of constitutional supercooling would not occur if the initial concentration of solution is lower and this condition does not encourage formation of dendritic ice crystals which normally trap the solutes between its structures and creating a lower concentration of ice layer (Miyawaki, 2018).

Additionally, effect size of this study was reported as eta-squared. Stirrer speed is deemed as having the highest impact on the TPC

increment as given by highest linear eta-squared (0.2689), followed by coolant temperature (0.1657), operation time (0.0598) and initial concentration (0.0476). It can be seen that the large effects ($\eta^2 > 0.14$) on TPC increment were provided by the stirrer speed and coolant temperature (Cohen, 1988). Concurrently, the medium effects ($0.06 < \eta^2 < 0.14$) were only contributed by the quadratic term of coolant temperature. It is also interesting to note that, even if the coolant temperature and stirrer speed were found to both give large effects on TPC increment at their linear term, their interaction term gave only a small effect size of 0.0242 ($0.01 < \eta^2 < 0.06$).

3.5. Optimum condition verification

Based on multi-response optimization, the produced 3D response surface plots successfully visualize the influence of coolant temperature, stirrer speed, operation time and initial concentration adopted in this study. The interactions phenomena between variables could be explicitly described by the multiple effects of solute concentration efficiency at appropriate combinations of operating conditions and an increase of ice crystallization surface area between the coolant and the juice solution for better mass and heat transfers. One optimal set of PFC conditions was achieved, i.e. -10.7 °C for coolant temperature, 400 rpm for stirrer speed, 35 min for operation time, and 6 mg/ml for initial concentration. The determination of the optimal conditions and predicted values for two responses was based on the overall desirability function of 0.92. Desirability or the objective function is an approach response transformation into a desired scale value, which widely used in the multi-response optimization. Thus, the overall desirability value can only be close to 1 if all of the responses are close to their optimal values (Akca and Anagun, 2013). Moreover, the multi-response optimization represents the relationship of all responses that must be simultaneously optimized, thus the costs can be reduced while improving the process efficiency and product quality.

From experimental validation process, the actual data obtained for K -value was 0.381, compared to the predicted value of 0.358. Concurrently, the experimental data of TPC increment was found to be 30.13% compared to the predicted value of 30.02% at the predicted optimum conditions. Thus, the percentage error for K -value and TPC increment are 6.42% and 0.37%, respectively, which are well within the satisfactory limits for low acceptable error. This allows for an inference that the models generated using MPCC crystallizer is highly satisfactory to generate the optimum conditions of cucumber juice concentration. It is noteworthy that the tested working conditions of PFC are seemingly more efficient by obtaining lower K -values combined with preserving the high TPC amount during the process. In short, a multi-response optimization study is more favored by manufacturers due to mimicking the real-life problems at the production scale.

4. Conclusions

The maximum improvement of ice crystallization surface area of MPCC crystallizer was 50.45% compared to a conventional PFC, which promotes better heterogenous nucleation and subsequent efficient ice crystal growth. The high surface area also gave 35.44% improvement in terms of productivity compared to the conventional design. By calculating the shape factor and mixing power consumption, the design features of the new PFC were ascertained to be within the standard ratio to give effective mixing and fluid movement for concentration purpose. With the aim to preserve the total phenolic compounds (TPC) at the highest, the regression models based on CCD by RSM were applied to optimize the PFC process, a non-thermal treatment. The multi-response optimization had been successfully utilized in this study to solve the multi-response surface problems, which is important to be considered at the production scale. Optimal values must involve more than one response in order to reduce costs and have more effective ways of concentration process while improving the product quality and quantity.

The experimental values are in agreement with the predicted values with optimal values obtained for *K*-value of 0.381 and TPC increment of 30.13%. It is confirmed once again that for this MPCC crystallizer, the PFC system performs better at moderate operating conditions of the studied factors. The high efficiency of retentions of the desired compounds in cucumber juice was successfully obtained in terms of purity of ice crystal and ice-liquid interface mass transfer. It can be concluded that this carefully designed MPCC can provide a PFC process with more efficient heat transfer and it can be a suitable option in enhancing the concentration of cucumber juice into a sophisticated process that fits the requirements of both industry and consumer. The study outcomes could help manufacturers commercialize this new technology in concentrating vegetable juices using an improved and unique design of non-thermal processing instead of the current thermal processing. Aside from minimizing the detrimental effects on nutrients in juices, this suggested that the design features should be of concerns in the production scale of food industries due to the complexity of this area subjected to the PFC geometry and fluid dynamic affects towards the ice growth rate.

CRedit authorship contribution statement

Nur Nabilah Hanani Mohd Rosli: Data curation, Writing – original draft. **Noor Hafiza Harun:** Software, Writing – original draft. **Roshanda Abdul Rahman:** Visualization, Investigation. **Norzita Ngadi:** Software, Validation. **Shafirah Samsuri:** Software, Writing – original draft. **Nurul Aini Amran:** Data curation, Writing – original draft. **Nor Zanariah Safiei:** Visualization, Investigation. **Farah Hanim Ab Hamid:** Formal analysis. **Zaki Yamani Zakaria:** Formal analysis. **Mazura Jusoh:** Conceptualization, Methodology, Writing – review & editing.

Declaration of competing interest

The authors declare that they have no known competing financial interests or personal relationships that could have appeared to influence the work reported in this paper.

Acknowledgements

The authors gratefully appreciate the support from Universiti Teknologi Malaysia under Collaborative Research Grant (CRG) (Vot no.: 08G23) and UTM Prototype Research Grant (Vot No.: 00L26). We are also indebted to Advanced Materials and Separation Technologies (AMSET) laboratory and Centre of Lipids Engineering and Applied Research (CLEAR), UTM Skudai in providing the facilities and infrastructures that permit us to run all experimental works.

Appendix A. Supplementary data

Supplementary data to this article can be found online at <https://doi.org/10.1016/j.jclepro.2021.129705>.

References

- Abbas, M., Saeed, F., Anjum, F.M., Afzaal, M., Tufail, T., Bashir, M.S., Ishtiaq, A., Hussain, S., Suleria, H.A.R., 2017. Natural polyphenols: an overview. *Int. J. Food Prop.* 20 (8), 1689–1699.
- Agatemor, U.M., Nwodo, O.F.C., Anosike, C.A., 2018. Phytochemical and proximate composition of cucumber (*Cucumis sativus*) fruit from Nsukka, Nigeria. *Afr. J. Biotechnol.* 17 (38), 1215–1219.
- Amran, N.A., Samsuri, S., Safiei, N.Z., Zakaria, Z.Y., Jusoh, M., 2016. Review: parametric study on the performance of progressive cryo-concentration system. *Chem. Eng. Commun.* 203 (7), 957–975.
- Akçay, H., Anagun, A.S., 2013. Multi-response optimization application on a manufacturing factory. *Math. Comput. Appl.* 18 (3), 531–538.
- Auleda, J.M., Raventos, M., Sanchez, J., Hernandez, E., 2011. Estimation of the freezing point of concentrated fruit juices for application in freeze concentration. *J. Food Eng.* 105, 289–294.
- Basli, A., Belkacem, N., Amrani, I., 2017. Chapter 10, Health Benefits of Phenolic Compounds against Cancers, *Phenolic Compounds – Biological Activity*, pp. 193–210.
- Birmingham, S.K., Neumann, A.M., Kramer, H.J.M., Verheijen, P.J.T., van Rosmalen, G.M., Grievink, J., 2000. A design procedure and predictive models for solution crystallisation process. *AIChE Symposium Series* 323 (96), 250–264.
- Bevilacqua, A., Petrucci, L., Perricone, M., Speranza, B., Campaniello, D., Snigaglia, M., Corbo, M.R., 2017. Nonthermal Technologies for fruit and vegetable juices and beverages: overview and advances. *Compr. Rev. Food Sci. Food Saf.* 17 (1), 2–62.
- Bhattacharjee, C., Saxena, V.K., Dutta, S., 2019. Novel thermal and non-thermal processing of watermelon juice. *Trends Food Sci. Technol.* 93, 234–243.
- Chandra, S., Khan, S., Avula, B., Lata, H., Yang, M.H., ElSohly, M.A., Khan, I.A., 2014. Assessment of total phenolic and flavonoid content, antioxidant properties, and yield of aeroponically and conventionally grown leafy vegetables and fruit crops: a comparative study. *Evid. base Compl. Alternative Med.* 1–9.
- Cohen, J., 1988. *Statistical Power Analysis for the Behavioral Sciences*, second ed. Erlbaum, Hillsdale, NJ.
- Ding, Z., Qin, F.G.F., Yuan, J., Huang, S., Jiang, R., Shao, Y., 2019. Concentration of apple juice with an intelligent freeze concentrator. *J. Food Eng.* 256, 61–72.
- Fellows, P.J., 2017. Chapter 13, evaporation and distillation, chapter. In: Fellows, P.J. (Ed.), *Food Processing Technology*, fourth ed. Woodhead Publishing, pp. 623–658.
- Gulfo, R., Auleda, J.M., Moreno, F.L., Ruiz, Y., Hernandez, E., Raventos, M., 2013. Multi-plate freeze concentration: Recovery of solutes occluded in the ice and determination of thawing time. *Food Sci. Technol. Int.* 20 (6), 405–419. <https://doi.org/10.1177/1082013213489127>.
- Hamid, F.H.A., Zakaria, Z., Ngadi, N., Jusoh, M., 2015. Application of progressive freeze concentration for water purification using rotating crystallizer with anti-supercooling holes. In: *Proceedings of 2015 5th International Conference on Environment Science and Engineering*.
- Isa, A.A., Samsuri, S., Amran, N.A., 2019. Integration of maceration and freeze concentration for recovery of vitamin C from orange peel waste. *IOP Conf. Ser. Earth Environ. Sci.* 268 (1), 1–7.
- Jia, H., Wang, H., 2021. Introductory chapter: studies on cucumber. *IntechOpen* 1–8. <https://doi.org/10.5772/intechopen.97360>.
- Kashid, M., Renken, A., Kiwi-Minsker, L., 2011. Mixing efficiency and energy consumption for five generic microchannel designs. *Chem. Eng. J.* 167 (2), 436–443.
- Kumar, V., Kaur, J., Gat, Y., Chandel, A., Suri, S., Panghal, A., 2017. Optimization of the different variables for the development of a cucumber-based blended herbal beverage. *Beverages* 3 (50), 1–13.
- Levine, T.R., Hullett, C.R., 2002. Eta squared, partial eta squared, and misreporting of effect size in communication research. *Hum. Commun. Res.* 28 (4), 612–625.
- Liu, J., Bi, J., McClements, D.J., Liu, X., Yi, J., Lyu, J., Zhou, Mo, Verkerk, R., Dekker, M., Wu, X., Liu, D., 2020. Impacts of thermal and non-thermal processing on structure and functionality of pectin in fruit- and vegetable-based products: a review. *Carbohydr. Polym.* 250 (116890), 1–14.
- Liu, L., Miyawaki, O., Hayakawa, K., 1999. Progressive freeze-concentration of tomato juice. *Food Sci. Technol. Res.* 5 (1), 108–112.
- Liu, L., Miyawaki, O., Nakamura, K., 1997. Progressive freeze-concentration of model liquid food. *Food Sci. Technol. Int. Tokyo* 3, 348–352.
- Lutz, M., Fuentes, E., Avila, F., Alarcon, M., Palomo, I., 2019. Roles of phenolic compounds in the reduction of risk factors of cardiovascular diseases. *Molecules* 24 (366), 1–15.
- Mallik, J., Akhter, R., 2012. Phytochemical screening and in-vitro evaluation of reducing power, cytotoxicity and anti-fungal activities of ethanol extracts of *Cucumis sativus*. *Int. J. Pharmaceut. Biol. Arch.* 3 (3), 555–560.
- McCabe, W.L., Smith, J.C., Harriott, P., 2001. *Unit Operation of Chemical Engineering*. McGraw-Hill, New York.
- Miyawaki, O., Lui, L., Nakamura, K., 1998. Effective partition constant of solute between ice and liquid phases in progressive freeze-concentration. *J. Food Sci.* 63 (4), 1–3.
- Miyawaki, O., 2018. Water and Freezing in Food. *Food Sci. Technol. Res.* 24 (1), 1–21. <https://doi.org/10.3136/fstr.24.1>.
- Miyawaki, O., Gunathilake, M., Omote, C., Koyanagi, T., Sasaki, T., Take, H., Matsuda, A., Ishisaki, K., Miwa, S., Kitano, S., 2016. Progressive freeze-concentration of apple juice and its application to produce a new type apple wine. *J. Food Eng.* 171, 153–158.
- Miyawaki, O., Inakuma, T., 2020. Development of Progressive Freeze Concentration and Its Application: A Review. *Food Bioprocess Technol.* 14, 39–51. <https://doi.org/10.1007/s11947-020-02517-7>.
- Miyawaki, O., Kato, S., Watabe, K., 2012. Yield improvement in progressive freeze-concentration by partial melting of ice. *J. Food Eng.* 108, 377–382. <https://doi.org/10.1016/j.jfoodeng.2011.09.013>.
- Miyawaki, O., Liu, L., Shirai, Y., Sakashita, S., Kagitani, K., 2005. Tubular ice system for scale-up of progressive freeze-concentration. *J. Food Eng.* 69, 107–113.
- Petzold, G., Orellana, P., Moreno, J., Cerda, E., Parra, P., 2016. Vacuum-assisted block freeze concentration applied to wine. *Innovat. Food Sci. Emerg. Technol.* 36, 330–335.
- Rastogi, N.K., 2016. Opportunities and challenges in application of forward osmosis in food processing. *Crit. Rev. Food Sci. Nutr.* 56 (2), 266–291.
- Safiei, N.Z., Ngadi, N., Johari, A., Zakaria, Z.Y., Jusoh, M., 2016. Grape juice concentration by progressive freeze concentrator sequence system. *J. Food Process. Preserv.* 1–12, 00.
- Saidu, A.N., Oibokpa, F.I., Olukotun, I.O., 2014. Phytochemical screening and hypoglycemic effect of methanolic fruit pulp extract of *Cucumis sativus* in alloxan induced diabetic rats. *J. Med. Plants Res.* 8 (39), 1173–1178.
- Samsuri, S., Amran, N.A., Jusoh, M., 2015. Spiral finned crystallizer for progressive freeze concentration process. *Chem. Eng. Res. Des.* 104, 280–286.
- Samsuri, S., Amran, N.A., Yahya, N., Jusoh, M., 2016. Review on progressive freeze concentration designs. *Chem. Eng. Commun.* 203 (3), 345–363.

- Samsuri, S., Amran, N.A., Jusoh, M., 2018. Optimization of progressive freeze concentration on apple juice via response surface methodology. *IOP Conf. Ser. Mater. Sci. Eng.* 358, 1–7, 012042.
- Santana, T., Moreno, J., Petzold, G., Santana, R., Saez-Trautmann, G., 2020. Evaluation of the temperature and time in centrifugation-assisted freeze concentration. *Appl. Sci.* 10 (9130), 1–11.
- Wang, Y., Lomakin, A., Latypov, R.F., Laubach, J.P., Hideshima, T., Richardson, P.G., Munshi, N.C., Anderson, K.C., Benedek, G.B., 2013. Phase transitions in human IgG solutions. *J. Chem. Phys.* 139 (12), 121904.
- Wu, Y.-Y., Xing, K., Zhang, X.-X., Wang, H., Wang, Y., Wang, F., Li, J.-M., 2017. Influence of freeze concentration technique on aromatic and phenolic compounds, color attributes, and sensory properties of cabernet sauvignon wine. *Molecules* 22, 1–18.
- Xie, M.H., Zhou, G.Z., Xia, J.Y., Zou, C., Yu, P.Q., Zhang, S.L., 2011. Comparison of power number for paddle type impellers by three methods. *J. Chem. Eng. Jpn.* 44 (11), 840–844.
- Yahya, N., Ismail, N., Zakaria, Z.Y., Ngadi, N., Rahman, R.A., Jusoh, M., 2017. The effect of coolant temperature and stirrer speed for concentration of sugarcane via progressive freeze concentration process. *Chem. Eng. Trans.* 56, 1147–1152.
- Yahya, N., Aziz, N.S., Nasir, M.Z., Zakaria, Z.Y., Ngadi, N., Jusoh, M., 2019. Heat transfer analysis on progressive freeze concentration of aqueous lysozyme solution. *Chem. Eng. Trans.* 72, 133–138.
- Yunusa, A.K., Dandago, M.A., Ibrahim, S.M., Abdullahi, N., Rilwan, A., Barde, A., 2018. Total phenolic content and antioxidant capacity of different parts of cucumber (*Cucumis sativus* L.). *Acta Univ. Cibiniensis. Ser. E Food Technol.* 22 (2), 13–20.
- Zhang, Z., Liu, X.-Y., 2018. Control of ice nucleation: freezing and antifreeze strategies. *Chem. Soc. Rev.* 47 (18), 7116–7139.